Research article

Hyperbranched polyethylenimine-modified polyethersulfone (HPEI/PES) and nAg@HPEI/PES membranes with enhanced ultrafiltration, antibacterial, and antifouling properties

Hussein K. Okoro [a,c,*], Lwazi Ndlwana [b], Monisola I. Ikhile [d], Tobias G. Barnard [e], J. Catherine Ngila [a,f]

[a] Analytical-Environmental, Membrane Nanotechnology Research Group, Department of Chemical Sciences, University of Johannesburg, P.O. Box 17011, Doornfontein 2028, Johannesburg, South Africa
[b] Institute for Nanotechnology and Water Sustainability (iNanoWS), College of Science, Engineering, and Technology, University of South Africa, Florida, Science Campus, P.O. Box 392, Pretoria 003, South Africa
[c] Environmental-Analytical Research Group, Department of Industrial Chemistry, Faculty of Physical Sciences, P.M.B. 1515, University of Ilorin, Ilorin, Nigeria
[d] Drugs Discovery and Smart Materials Research Group, Department of Chemical Sciences, University of Johannesburg, P.O. Box 17011, Doornfontein 2028, Johannesburg, South Africa
[e] Water and Health Research Centre, University of Johannesburg, Doornfontein Campus, South Africa
[f] The African Academy of Sciences, P.O. Box 24916-00502, 8 Miotoni Lane, Karen, Nairobi, Kenya

HIGHLIGHTS

- New flat sheet membranes possessing both organic antifouling and antibacterial properties were fabricated.
- The successive modification of PES with HPEI and nAg resulted in enhanced membrane properties.
- Most of the membranes exhibited good antibacterial activities against the bacterial strains tested.
- Membrane samples with nAg also displayed good antibacterial activities against bacteria E Coli.
- The use of cost friendly HPEI and low levels of modification, and ease of membrane fabrication was achieved.

ARTICLE INFO

ABSTRACT

This study reports a simple fabrication of polyethersulfone (PES)-based membranes, their characterisation, and application. These membranes are modified with hyperbranched polyethyleneimine (HPEI) and -silver (nAg)-decorated HPEI. These were then compared for filtration, organic fouling, antifouling, and antibacterial properties against the neat PES membrane. The fabricated membranes were characterised for their chemistry using attenuated transmission reflectance-equipped Fourier transform infrared spectroscopy (ATR-FTIR) and x-ray photo-electron spectroscopy (XPS). As such, the presence of HPEI interactions between the nAg and HPEI in the membranes was confirmed. An energy-dispersive x-ray detector coupled with a scanning electron microscopy (SEM-EDS) and atomic force microscopy (AFM) were used to study morphological, compositional, topographical, and topological changes to the membrane due to the modifications. A thermogravimetric analyser (TGA) was also utilised to evaluate the effect of modification on thermal stability of the resulting membranes. Optical contact angle (OCA) interrogated the extent of membrane/water interactions which indicated enhanced hydrophilicity due to the modification. Dead-end filtration using these membranes indicated enhanced pure water permeate fluxes and protein rejection (bovine serum albumin, BSA). The results of the BSA rejection for the HPEI/PES membranes were a maximum of 98% while those of the nAg@HPEI/PES ranged between 30-87%. The membranes possessed high flux recoveries, indicating great potential for the membranes for antifouling applications in water treatment. Extensive antibacterial studies were carried out on the membranes to probe bioactivity. Enhanced activity was recorded (except for neat PES) with zone inhibitions of up to 7 mm against five bacterial strains including *E. Coli* and *K. Pneumoniae* as found in several wastewater streams. The antibacterial properties of

---

* Corresponding author.
E-mail addresses: okoro.hk@unilorin.edu.ng, hkoadeola@gmail.com (H.K. Okoro).

these membranes mean they can prolong membrane operational lifetime by mitigating biofilming during water treatment.

1. Introduction

Water is a useful and valuable resource for human existence. The lack of sufficient potable water has led to many people to depend on rivers for drinking and other domestic use [1].With the growing or rapid industrialization, significant amounts of organic and inorganic pollutants have been deposited into water bodies and soils and this discharge resulted in their massive pollution. consequently endangering human health [2]. More than 3.6 million people worldwide die annually owing to the consumption of unsafe water. The lack of access to good quality water has remained one of the most critical challenges facing mankind around the globe. As a result, many technologies have been introduced to tackle water issues and increase the availability of potable and non-potable water [3, 4, 5].

Various technologies have been employed for wastewater treatment. These include chemical precipitation, coagulation-flocculation, ion-exchange, adsorption, evaporation, biosorption, and membrane filtration. There are many advantages of membrane technology over other techniques and these include high separation efficiency, no phase changed involved, eco-friendly, ease of operation, and scale up, energy saving [6]. The introduction of polymeric membrane technology has been useful in solving problems related to wastewater treatment. The advantages of membrane technology include cost, less chemical consumption, and small footprints, among others. Ultrafiltration (UF) is one of the useful membrane separation processes aptly applied in various areas such as wastewater reuse, borehole water, and wastewater treatment [7]. As such, several countries especially in the Middle and Far East have adopted polymeric membranes to produce drinking water and to purify industrial effluents [8, 9, 10].

However, polymers widely used in the preparation of polymeric membranes such as polyvinylidene difluoride (PVDF) and PES possess notably hydrophobic properties. This limits their application in water treatment as hydrophobic interactions with natural or biological organic matter (NOM and BOM) in water are promoted. The upshot is then a process called fouling where a build-up of these unwanted materials occurs on the membrane surface and pores, restricting water transport, which and increases operational pressure requirements, and shortens membrane lifespan [11, 12]. Both increased operational pressure and frequent membrane cleaning drive up operational costs, and hence membranes need to be modified to improve hydrophilicity. Hydrophilic membranes achieve excellent use in water treatment application by mitigating the loss of water, lowering input energy, and driving down operational and maintenance costs [13, 14, 15]. Several methods have been proposed for membrane modification. These include surface (chemical) grafting of various hydrophilic/amphiphilic monomers/polymers or biomolecule through a redox reaction, irradiation, and/or blending. Most of these methods demonstrate that modified membranes show improved water permeability and reduced fouling by proteins owing to the enhanced hydrophilicity. It is also important to modify membrane with a self-antibacterial property to inhibit bacteria growth and development of biofilm (biofouling). As previously mentioned, these can also be achieved by using surface modification blending methods. It is to be noted that blending has the advantage of easy precipitation through phase inversion [16, 17]. However, long term leaching of strictly hydrophilic modifiers may occur. As such, blended hydrophilic ligands can also be crosslinked to mitigate leaching as carried out by Chen et al (2018). The authors herein, incorporated an amphiphilic polymer (polyethyleneimine) which was subsequently crosslinked with tannic acid (TA) [18]. The benefit of the said approach is that the crosslinking/quartenisation greatly minimizes the leaching of the PEI. The

only drawback is the previously reported pore blockage and film formation to the existing membrane during crosslinking, and thus reduced permeation. This is all due to the problems caused by post-modification of membranes by polymers [6]. However, when high molecular weight amphiphilic polymers such as HPEI are only physically blended into the polymer casting solution, the coagulation process controls pore formation. This is because such polymers possess both hydrophobic and hydrophilic tail ends) [19]. Furthermore, nanoparticles such as Ag or its oxides can be added to improve water interactions, biogenicity, permeate fluxes, and antifouling.

In the literature, silver nanoparticles (nAg) have been widely used as effective antibacterial agent owing to its excellent antibacterial property. Zodrow and co-workers (2009) prepared nAg-incorporated into polysulfone ultrafiltration membranes (nAg PSF) via wet phase inversion. Their findings showed that membrane formed exhibited antibacterial properties towards different bacteria [20]. Silver ions can be reduced into silver nanoparticles by polyvinylpyrollidone (PVP) and can also enhance distribution of silver nanoparticles in the polymer matrix [19, 21].One must be mindful, however, of metal leaching which can introduce secondary pollution when the nanoparticles are not strongly (mostly chemically) bound to the membrane matrix. As such, Prince *et al.*, (2014) synthesized self-cleaning metal organic framework (MOF)-based ultrafiltration membrane which displayed enhanced antifouling and bacterial inhibition properties [22]. Multifunctional macromolecules and dendritic polymers such as hyperbranched polyethyleneimine (HPEI) have be exploited to anchor nanoparticles onto and within the membrane matrix. The anchoring of nanoparticles to the membrane matrix is not the only advantage that HPEI offers. HPEI, just like nAg possesses antibacterial properties where its hydrophobic side can penetrate and break microbial cell walls, promoting cytotoxity. Additionally, it can mitigate the formation of biofilms thus imparting antifouling properties [23].

Based on the above, it can be seen how the synergistic properties of nAg and HPEI are interrogated in a PES nanocomposite membrane. The effect of amphiphilic HPEI on the filtration and antibacterial/antifouling performance of formed membranes was investigated. This is because of the scarce literature for the exploitation of the antibacterial and anti-biofouling properties of HPEI. The said properties as imparted by HPEI are to be compared against those of nAg as anchored onto HPEI in the PES membrane matrix. Pure water flux, BSA rejection, irreversible flux recovery and contact angle were also studied. The antibacterial properties of HPEI and nAg in the membranes will be compared using five bacterial strains as commonly found in South African wastewaters.

2. Materials and methods

2.1. Materials

Polyethersulfone (PES) 3100P (powder, Mw. 30–55 kDa) (Solvay, Belgium). *N*-methyl-2-pyrolidone anhydrous (NMP, 99.8%), polyvinlpyrolidone (PVP, Mw. 40 KDa) and hyperbranched polyethylenimine (HPEI) (Mw. ~25 kDa, silver nitrate (solid, AgNO₃, 99%), ethanol (99.5%), acetone (99.5%), and bovine serum albumin (BSA) were all purchased from Sigma Aldrich, South Africa. All these reagents were used without further purification. A 3520 Baker film applicator casting knife (Elcometer, Germany) was purchased from Bengatouch, South Africa. The five strains of bacteria used were namely *E. coli*, *K. pneumoniae*, *S. aureus*, *P. aeruginosa*, and *E. faecalis* were obtained from the American Type Culture Collection (ATCC, USA). The water used for all experiments was obtained from the Millipore (Japan) RO system.

2.2. Method

2.2.1. Preparation of the casting solutions

The PES powder was dried at 110 °C for 12 h before use The PES and HPEI/PES casting solutions were prepared as follows: 3.6 g PES was completely dissolved in NMP (16.5 g) at 60 °C and then 0.05 g PVP powders and the HPEI amounts varied from 0% to 3%. The solutions were then rested for up to 24 h to degas before casting and subsequent phase inversion.

2.2.2. Membrane fabrication

The degassed casting solution was spread on a clean glass plate with a casting knife with a gap set at 250 μm. The casted liquid film was evaporated in air for 20 s and then immersed in a water coagulation bath for 24 h.

2.2.3. Modification of the membranes with nAg

To embed the nAg, a 1 m/m% solution of $AgNO_3$ was prepared in a mixture of 90:10 v/v% ethanol/water. The 5.02 cm diameter membranes were subsequently immersed into the solutions for 10 minutes. The latter were then abundantly washed in an ethanol/water mixture and then dried at room temperature for characterisation.

2.3. Characterisation

To embed the nAg, a 1 m/m% solution of $AgNO_3$ was prepared in a mixture of 90:10 v/v% ethanol/water.The 5.02 cm diameter membranes were subsequently immersed into the solutions for 10 min. The latter were then abundantly washed in an ethanol/water mixture and then dried at room temperature for characterisation.

2.3.1. Scanning electron microscopy (SEM)

For surface analysis, the dried membranes were cut into 1 cm × 1 cm square pieces. The membrane samples designated for cross-sectional analysis were prepared byimmersing and fracturing them in liquid nitrogen to reveal the internal-structure. The samples were then coated using the Q150TE (Quorum, U.K.) carbon coater before the samples were observed by SEM (TESCAN, Czech Republic) at an accelerating voltage of 10 kV controlled by the Vega 3Xmn software. The elemental composition of the membranes was obtained using an energy dispersive detector (EDS) controlled by the INCA software (Oxford Instruments, U.K).

2.3.2. Atomic force microscopy (AFM)

The membrane surfaces were characterized for surface roughness, topology, and topography using the Nanoscope IV controller (AFM, Veeco, USA) non-contact mode. The membranes were cut into 1 cm × 1 cm square pieces and placed onto carbon tape covered nickel sample holders and subsequently introduced to sample stage in the path of a silicon cantilever. The values of roughness were recorded over different areas of each membrane sample using non-contact mode to scan the membrane surfaces. Topographic images were taken at 5 μm resolution and used to calculate surface roughness (R_a), R_a and RMs R_q) are defined as roughness and dimension, respectively. Similar approaches have been previously reported [15].

2.3.3. Attenuated total reflectance-Fourier Transform infra-red (ATR-FTIR)

Prior to the spectra measurements, membranes were dried in a desiccator at room temperature. This was followed by recording their attenuated total reflectance-Fourier Transform infra-red (ATR-FTIR) spectra using the Spectrum 100 spectrometer (PerkinElmer, USA). The scanning range utilized was 650–4000cm^{-1} averaging 64 scans at a resolution of 4cm^{-1}.

2.3.4. X-ray photoelectron spectroscopy (XPS)

The XPS, Omicron Nanotechnology, Germany) was used to confirm the ATR-FTIR data of the dried membrane samples. The binding energies

(B.E) were calibrated to 284.6 eV (C 1s peak) and the analyses carried out at 1.8×10^{-8} Torr at an emission current of 15 mA. During the analysis, the sample substrates were flooded with electrons using the instrument's built-in neutralizer because of their electrically insulating nature.

2.4. Thermogravimetric analysis (TGA) thermal analysis

The TGA gave useful information about the weight change of the membrane samples as a function of temperature or time during heating. The HPEI/PES and nAg@HPEI/PES nanocomposite membrane was analysed using a differential scanning colorimetry-coupled thermogravimetric analyser (DSC-TGA, TA Instruments, USA) The samples were equilibrated at 25 °C–1000 °C, ramped at 10 °C min^{-1} purged in nitrogen environment N_2 flow rate at 100 ml/min, average sample mass used was 5–10 mg.

2.5. Contact angle measurements (OCA)

The contact angle of membranes was measured on a goniometer (OCA20, Data physics, Germany). A water droplet (5 μL) was lowered onto the membrane surface from a needle tip on dispensing syringe. A magnified image of the droplet was recorded by a digital camera as per other works [24, 25]. Static contact angles were determined from these images with automated software after every 30 s. The contact angles measurement was taken the mean value of 5 different points on each membrane.

2.6. Water flux, protein (BSA) rejection and flux analysis

The flat sheet membranes were conditioned at 200 kPa and then reduced to 100 kPa for flux measurement using a Sterlitech (USA) HP7450 stirred dead-end cell. The volume was recorded over 1-min periods thrice and the obtained value was computed as J_w (pure water flux) according to Eq. (1) [26, 27]:

$$J_w = \frac{Q}{A\Delta t} \tag{1}$$

where Q is the permeate volume, A the membrane effective area, and Δt is the permeate volume collection time.

The membranes were also evaluated for the rejection of BSA as model foulant by dead-end cell filtration. To carry out these experiments, a 1000 ppm (200 mL) BSA solution was prepared and subsequently added to the cell, similarly to other works in the literature [28]. The membrane was exposed to the BSA solution for 10 min followed by periodical sampling over an hour for the determination of BSA rejection according to Eq. (2):

$$R\% = \left(1 - \frac{C_p}{C_b}\right) \times 100 \tag{2}$$

where C_p and C_b are the respective concentrations of the permeate and retentate solutions. All experiments were conducted in triplicate to minimise associated errors.

2.7. Fouling studies

Fouling studies were also conducted to investigate the fouling propensity of the fabricated membranes. To determine this parameter, the membrane was exposed to the BSA solution in a dead-end cell over a period of an hour over 10 fouling cycles. The membrane was backwashed twice with deionised water. The membrane was then returned to the cell, passing deionised water again to measure the permeate and record fluxes as J_{w1} (similarly to Equation 1). All experiments were conducted in triplicate to minimise associated errors. The fluxes obtained from these experiments allowed for the computation of reversible flux ratios (FRR%) as per Eq. (3):

$$FRR(\%) = \frac{J_{wp}}{J_w} \times 100 \qquad (3)$$

2.8. Antibacterial activity of the membranes

2.8.1. Bacterial strains, Mueller Hinton broth, bacteriological agar, agar plates and agarose gel preparation

The five bacterial strains were diluted in saline to a 0.5 McFarland concentration using test tubes. A Mueller Hinton broth was weighed and dissolved in 200 mL water and autoclaved at 121 °C and 15 psi for 1 h. Bacteriological agar was prepared by weighing 0.21 g of 14 g/L and dissolved in 15 mL water and boiled and placed in a water bath at 50 °C. Mueller Hinton agar was prepared by weighing 7.6g of 18 g/L in 200 ml of water and boiled then autoclaved at 121 °C and 15 psi for 1 h and poured into petri dishes. The 1% agarose gel was prepared using 1g/100mL dissolved in Tris-acetate-EDTA (TAE) buffer and boiled. A minimum of three essays were carried out for each analysis under this subsection.

2.8.1.1. Media preparation and antibacterial tests. The five bacterial strains namely were diluted in a saline solution to a (0.5 McFarland turbidity standard) concentration using test tubes. Mueller Hinton broth was dissolved in 200 ml distilled water and autoclaved for 1 h. Bacteriological agar was prepared by weighing 0.21 g of 14 g/l and dissolved in 15 mL water and boiled and placed in a water bath at 50 °C. Mueller Hinton agar was prepared by weighing 7.6 g of 18 g/L in 200 ml of water and thus boiled then autoclaved at 121 °C and 15 psi for 1 h and poured into petri dishes. The 1% agarose gel was prepared using 10 g/L dissolved in tris acetate EDTA(TAE) buffer and boiled. Table 1 shows the information of all the bacterial strains used in this work.

2.8.1.2. Bacterial lawn and overlay. A 100 μL of each bacterial strain dilution previously prepared were pipetted and evenly spread onto five Mueller Hinton agar plates to form a bacterial lawn, a triplicate plate of six were made for each strain then allowed to dry. Only one plate of each strain was used and impregnated with blank and positive control antibiotic discs saturated in neomycin as well as four different membranes. The plates were then incubated at 37 °C for 24 h. A layer of 4 mL bacteriological agar was mixed with 1 mL for each of the bacterial strains; a layer for each bacterium was spread over the antibiotic disks for all the controls and onto the plates consisting of the membranes sprayed with silver nitrate and a control blank without any antibiotic. The plates were then allowed to set and incubated at 37 °C for 24 h.

2.8.1.3. Indicator of bacterial growth. To indicate bacterial growth, Kirby-Bauer tests aka zone of inhibition tests were carried out on the membrane samples using the said bacterial strains. A set of falcon tubes were placed into a test tube rack and into each tube, 0.5 mL of iodonitrotetrazolium chloride (INT) dye and 1.5 mL of double concentrated sim plate media was added. In a separate tube, 2 ml agarose was added and mixed with the INT mixture and pipetted onto the agar overlay plates that grew from the previous day by creating a thin layer over it, as not to disturb the bacteria. The plates were set and observed for any change in color, all plates were then incubated at 37 °C and checked at every 15 min intervals for color change and fluorescence and later at every 30 min

interval. Active bacterial cells reduce the INT to purple colour indicating bacterial survival and thus no inhibition.

2.8.1.4. Statistical analysis of data. The results obtained from this research were subjected to various statistical analyses using statistical package for social scientists (SPSS) software (version 23.0) and Microsoft ware Excel 2007 were also used for data analysis.
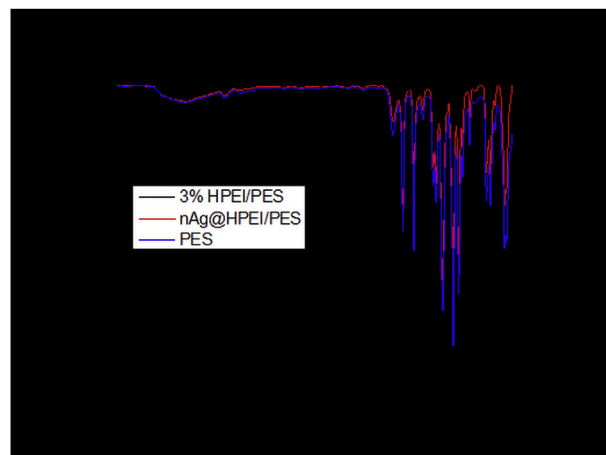
3. Results and discussion

3.1. Membrane characterization

3.1.1. Surface chemistry

The FTIR of the HPEI/PES and Ag@HPEI/PES was investigated. The neat PES membranes presented intrinsic PES bands at 1300–1320, and 1487 and 1578 cm^{-1} (Figure 1) corresponding to vibrations and stretches of the aromatic chains, respectively. Upon the addition of HPEI, the two latter bands formerly discussed could still be seen, but with greater intensity. This confirmed the weak interactions that occur between HPEI and PES. The same bands shift significantly to higher wave numbers upon the introduction of nAg owing to the steric effects of the heavy Ag atoms in the molecular structure of the HPEI/PES membrane matrix. Chemical interactions were then confirmed by the appearance of new and strong bands between 1680- 2200 cm^{-1}.

To corroborate the ATR-FTIR results, XPS analysis was also carried out for the membranes before and after modification. Figure 2 depicts the species present in the membrane due to this modification, comparing the spectra against the neat PES membranes. Figure 2a shows the C1s core level as could be deconvoluted to two components, the C–C/C–H and the C–O species which are typical of PES [15]. Upon the modification with HPEI and Ag NPs, the peak areas of the former respective peaks were enhanced. This can be attributed to the compositional contribution by carbon from HPEI which also introduces amine species. However, this C–NH$_2$ overlaps with the C–O at 285.7 eV, with another substituted amine appearing at 287.6 eV [29]. The O peak on Figure 2c indicated the typical large presence of ether groups belonging to PES (O–C- at 528.9 eV). The peak area of this O–C species was drastically reduced by the modification, also resulting in the new O–Ag peak showing at 528.7 eV as deconvoluted. This peak indicates the existence of molecular Ag due to oxidation. Entirely new N species from HPEI were also observed due to the modification and these assist in anchoring the Ag NPs. As such, the NH–Ag component at 398.4 eV was observed, indicating successful anchoring of the nAg onto the membrane matrix. Furthermore, two peaks belonging to nAg were detected on the membrane at binding energies of

Table 1. Detailed information about the five strains of bacteria used.

Organism	Abbreviation	ATCC #	Gram	Motile
Escherichia coli	E. coli	25922	Negative	Yes
Pseudomonas aeruginosa	P. aeruginosa	27853	Negative	Yes
Klebsiella pneumoniae	K. pneumoniae	13882	Negative	No
Staphylococcus aureus	S. aureus	1026	Positive	No
Enterococcus faecalis	E. faecalis	7080	Positive	Yes

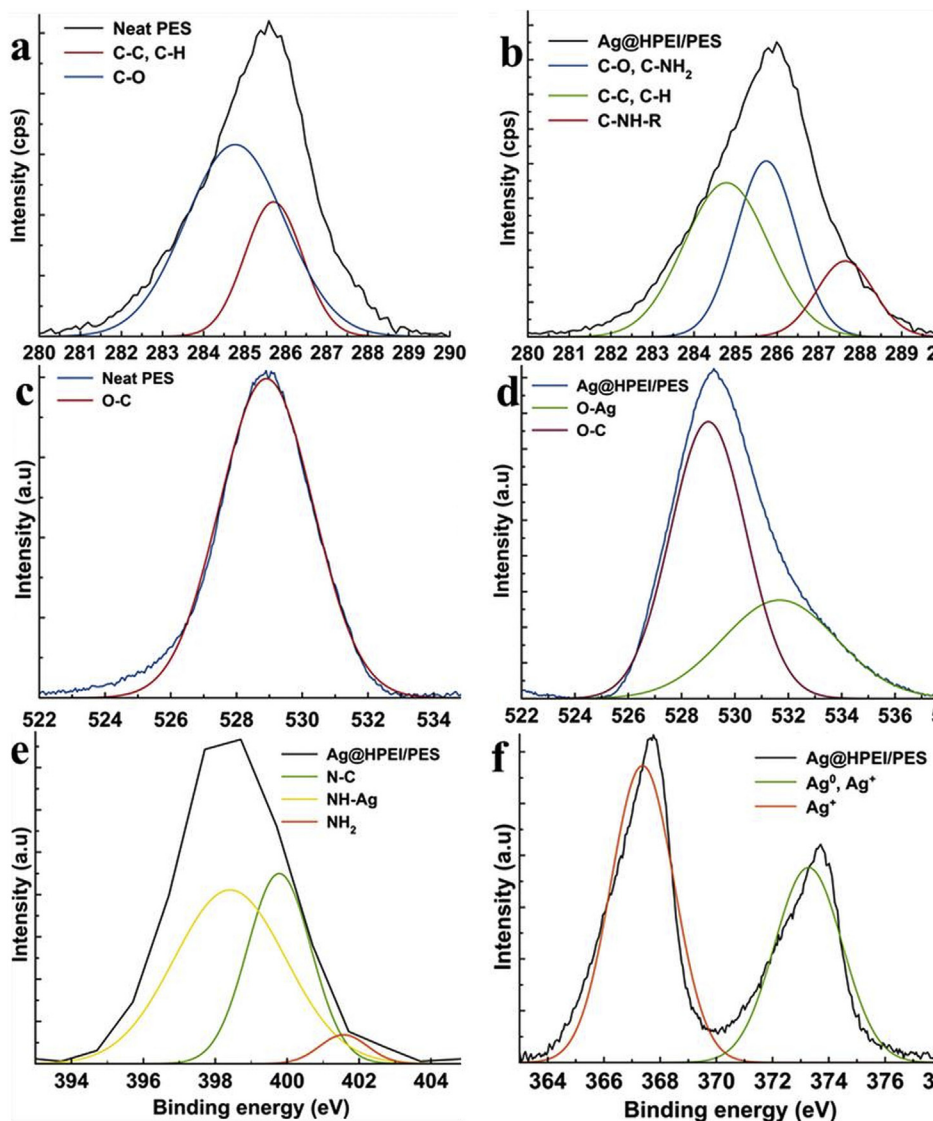**Figure 1.** ATR-FTIR spectra of the PES (red), 3% HPEI/PES (black), and nAg@HPEI/PES (blue).

Figure 2. XPS spectra for the neat and modified PES membranes.

367.4 eV and 373.3 eV, respectively assigned to the metallic and molecular Ag (Figure 2) [30].

Thermogravimetric analysis was also carried out for the membranes, and the TGA curves depicted in Figure 3. As can be observed on the thermogram in Figure 3a), neat PES presents its typical thermal stability where it only starts degrading at 489 °C. This is the point at which the oxygen-bonded functional groups of PES are lost. However, the introduction of HPEI does not improve thermal stability as the composite degrades at a lesser temperature as can also be observed for the nAg@HPEI/PES nanocomposite (491 and 401 °C respectively). The
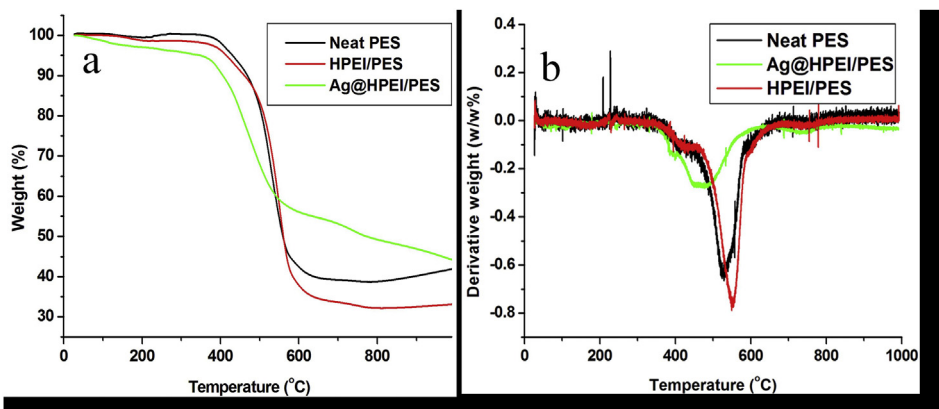

Figure 3. Neat PES, HPEI/PES, and Ag@HPEI/PES: (a) thermograms, and (b) first differential thermograms.
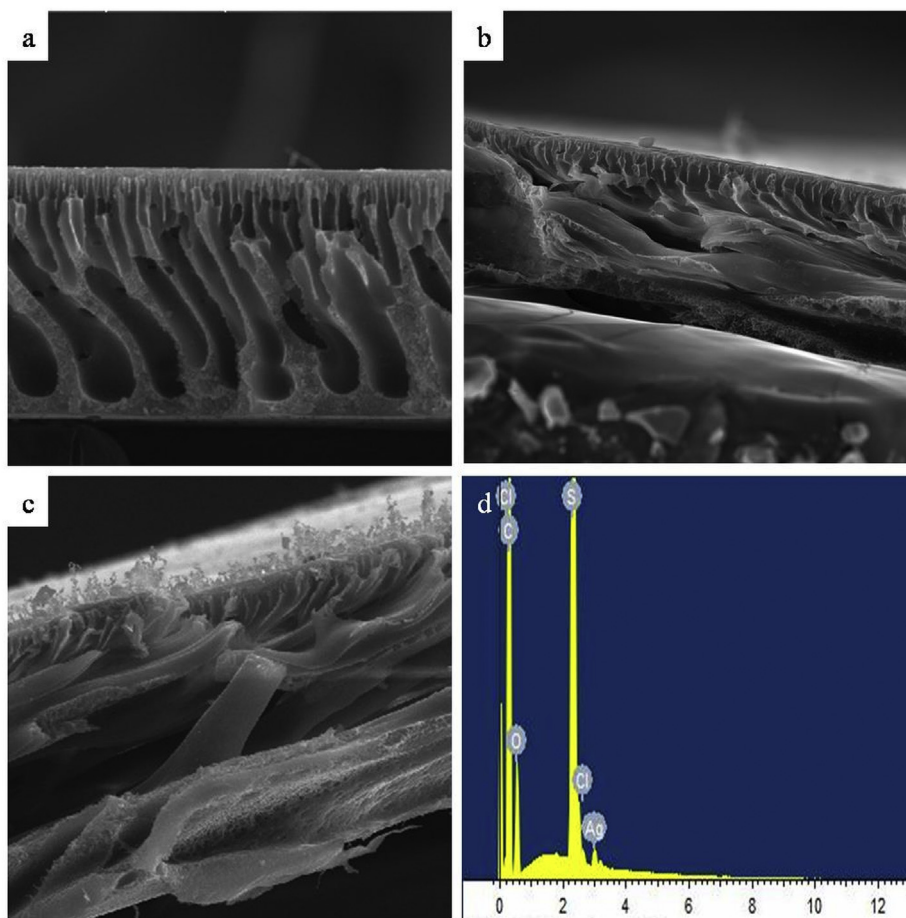
Figure 4. SEM cross-sectional membrane micrographs of neat PES (a), nAg@1% HPEI/PES, and nAg@3%HPEI/PES, and the EDS spectrum of nAg@3%HPEI/PES.

decrease in thermal stability can be attributed to amorphous nature of HPEI and the lack of chemical bonding between it and PES. Nonetheless, the expected membrane operational conditions will not be this harsh. As such, the decrease in thermal stability should not raise great concern. The first differential thermograms in Figure 3b) further describe the thermal behaviour of the membranes. It can be observed that the major chemical
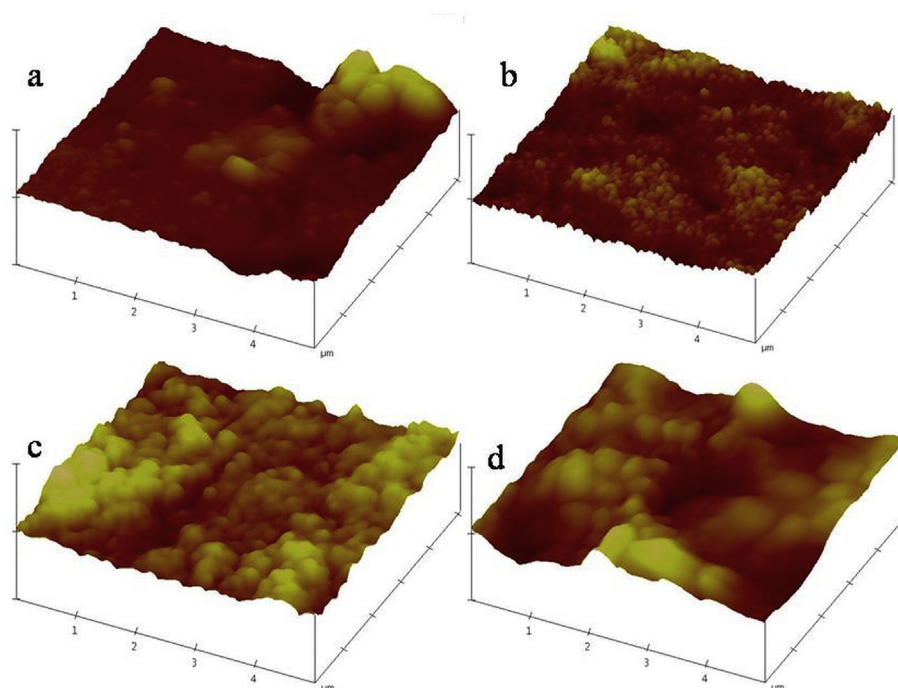
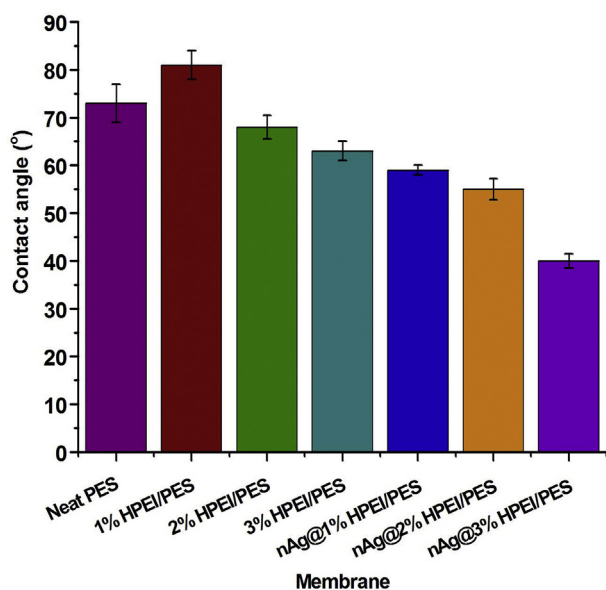**Figure 5.** AFM 3D micrographs for the fabricated membranes with increasing modification.

Figure 6. Optical contact angle measurements for the prepared membranes.

changes occur at the temperatures of 526, 551, and 478 °C for the respective membranes. These thermochemical changes are indicative of the chemical modification as observed on the ATR-FTIR and XPS spectra.

The surface morphology and the cross-section of the membranes were investigated using SEM as depicted on Figure 4. The synthesised membranes show different internal structure depending on their composition. The SEM images for neat membrane show fingerlike structure while that of HPEI/PES possessed clear macrovoids in its internal structure depending on their HPEI contents (shown herein is the nAg@1% HPEI/PES membrane. HPEI greatly contributed to the changes in the morphology of the membranes i.e. the structure changes from finger-like to macrovoids. This observation can be explained by the rapid liquid-liquid demixing of HPEI/PES in water owing to the compatibility of HPEI with water [31]). HPEI/PESs. The nAg@HPEI/PES membrane still possessed macrovoids mainly because the changes made to the HPEI/PES membrane was the chelation of the nAg. The surface of the membrane can also be seen possessing particulate material which was confirmed to be nAg by SEM-EDS (Figure 4d).
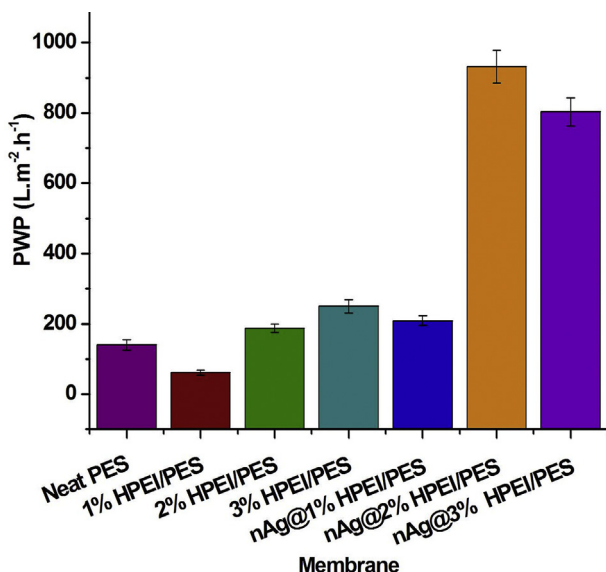
Morphological studies were also carried out using AFM to study topology and surface roughness as presented on Figure 5. It was observed that increasing the HPEI concentration resulted in greater surface roughness. The surface roughness observed for neat membrane was 10.874 nm with increasing modification, the values were recorded to be 14.494 nm, 62.594 nm and 19.128 nm respectively. The decreasing values in surface roughness similarly to the current work have been reported to enhance hydrophilicity and reduce foulant molecule-membrane interactions [32].

The contact angle measurements for all membranes were taken (Figure 6). The neat PES membrane presented a high contact angle owing to the relatively hydrophobic nature of PES. The 1% HPEI/PES membrane demonstrated light increase in the contact angle as compared to the pristine. However, lower contact angles were observed as the values decrease from the former 82–64° from 1 – 3% HPEI loading. For instance, on Figure 6, the OCA for neat PES is 73°. The error would then be + - 5° based on the error bars. The contact angle increased from 73+-5 degrees of the neat PES to 81+-3° for 1%HPEI/PES. However, with increasing modification, a decreasing trend was observed between 2%HPEI/PES until nAg@3%HPEI/PES from 68+-3° to 40 +-2°. The effects of HPEI on the contact angle of sulfone membranes has also been investigated by Vlotman et al (2018) where the structure of this molecule enhances water interactions through the hydrophilic terminal amine moieties [33]. Furthermore, the inclusion of nAg with the loading increments of HPEI resulted in decreasing contact angles to an ultimate of 38°. These observations indicate that the incremental modification with HPEI and nAg was successful. As such, the membranes have great potential of application in water treatment where antifouling properties are required. The topological and surface roughness trend observed for these membranes are in line with other works in literature [13].

3.2. Filtration experiments

3.2.1. Pure water permeation fluxes

The dead-end cell filtration was carried out on the membranes as demonstrated in Figure 7. The neat PES membranes indicated low fluxes. Upon the addition and increasing HPEI loading, a drastic flux improvement could be observed. This could be attributed to the hydrophilic segments of HPEI which enhance membrane-water interactions. The direct consequence of this was the improved solute transport which increased water permeate fluxes for the HPEI/PES membranes [34]. For the nAg@HPEI/PES nanocomposites, it can be observed that these
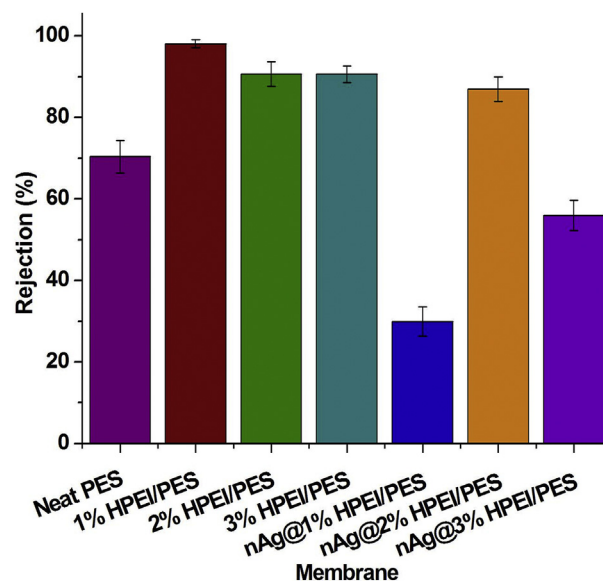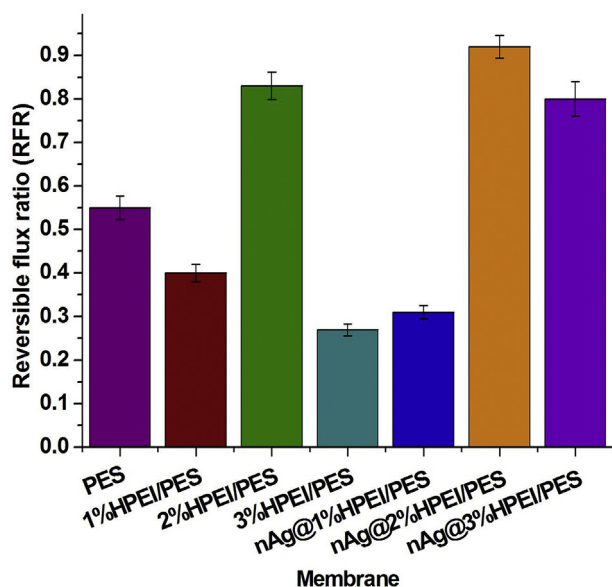

Figure 7. Pure water permeate fluxes for the prepared membranes.

Figure 8. Protein rejection by the prepared membranes.

Figure 9. RFR measurements for the prepared membranes.

3.2.2. BSA (protein) rejection

Protein rejection studies were also carried out to investigate the ultrafiltration properties of the newly fabricated membranes. The results can be observed on Figure 8 where low rejections by the neat PES membrane were recorded. The introduction of HPEI resulted in the highest rejections over the other membranes prepared, at 98%. This observation pointed at a trade-off between achieving protein rejection and PWP, of which the former was high, and the latter low. However, the nAg@1%HPEI/PES nanocomposite presented lowest protein rejections in all membranes prepared. When compared to others, the nAg@2% HPEI/PES membrane seemed to strike the greatest balance between protein rejection and PWP at 90.7% and 931 $L\,m^{-2}.h^{-1}$, respectively. The importance of achieving a balance between these two parameters has been previously highlighted by other authors [35].

3.2.3. Antifouling behaviour

Reversible flux ratios (RFR) were calculated for all the interrogated membrane samples as a measure of flux recovery and antifouling behaviour. As illustrated in Figure 9, the neat PES membrane indicated low RFR values. This can be attributed to the relative hydrophobic nature of PES and the recorded low PWP as previously discussed in Section 3.2.2. For the HPEI/PES membranes, the RFR values were recorded to be higher than those observed for neat PES. The reason for this was the inclusion of hydrophilic groups as found in the molecular structure of HPEI which increase water interactions and solute transport. This in turn reduces protein adherence onto the membranes and thus mitigates flux loss. The inclusion of nAg also resulted in enhanced antifouling properties with increasing HPEI loading as compared to samples with lower HPEI content. The increasing HPEI content also allows for improved nAg hosting capacities, resulting in the enhanced surface hydrophilicity and reduced protein adhesions between BSA and the nAg@HPEI-containing membranes [22].
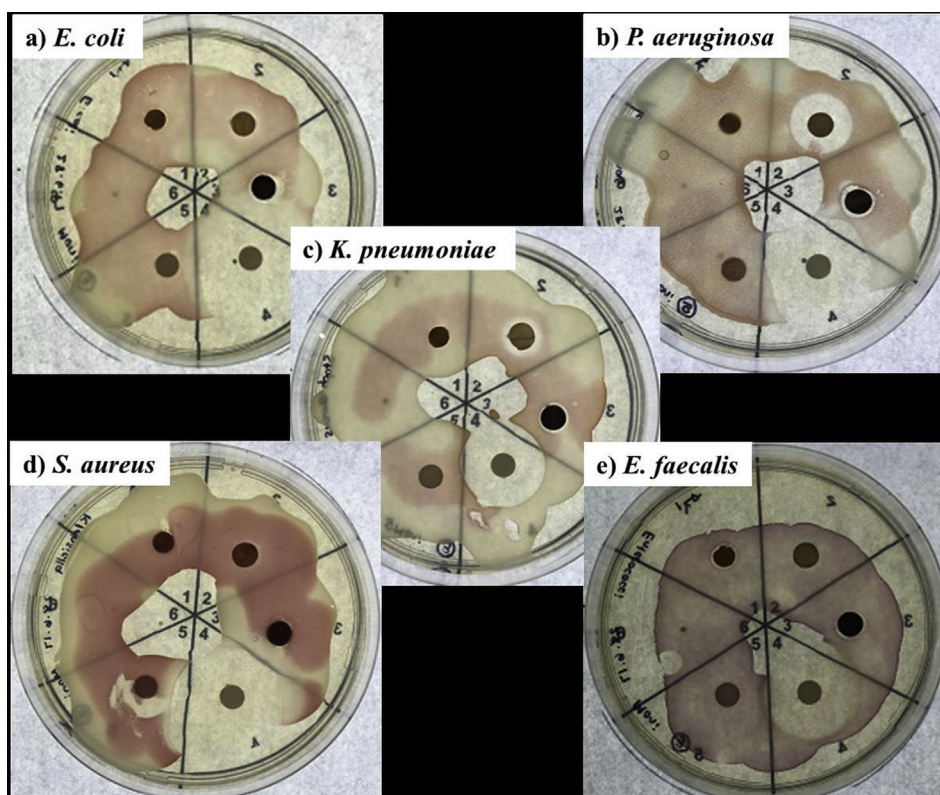
membranes possess the highest water flux values. This is also because of the further hydrophilicity improvement as imparted by the argentization of the HPEI/PES surface, agreeing with the work by Prince *et al.*, (2014). However, to obtain the highest fluxes, it is observable that the 2% HPEI/PES membrane resulted in the most optimum Ag chelation and thus the deposition of nAg on the membrane surface. Further than that, the observable fluxes decreased as there could have be an excess of nAg in the membrane matrix that impeded the water transport. These observations are similar in trend to Chen *et al.*, (2012) [13].

Figure 10. Representation of the zone of inhibition tests for the membranes against different strains of bacteria (with INT dye). On this figure are the 3rd plates containing the 3% permutations of modification.

Table 2. The average diameter of inhibition (in mm) for the membrane samples and the controls negative (blank) and positive (neomycin) against five bacterial strains.

Test compound	E. coli	P. aeruginosa	K. pneumoniae	S. aureus	E. faecalis
1%HPEI/PES	4	5	~	5	5
1%HPEI/PES	7	5	4	5	5
nAg@1%HPEI/PES	5	5	3	5	5
2%HPEI/PES	4	~	~	5	5
2%HPEI/PES	4	4	~	~	6
Ag@2%HPEI/PES	4	5	3	~	5
3%HPEI/PES	5	5	5	~	5
3%HPEI/PES	6	4	~	~	6
nAg@3%HPEI/PES	5	5	~	6	6
Blank	~	~	~	~	~
Neomycin	24	24	25	21	23

~: no activity was recorded.

3.3. Antibacterial interrogation: zone inhibition tests

According to the results shown in Figure 10, as directly read from the plate, the blank (labelled 5) without antibiotic shows no inhibition zone on the surface and around it. In fact, the blanks were completely covered by the test microorganisms. On the contrary, the control (labelled 4) which was layered with antibiotic (neomycin) shows significant inhibition zone on the surface and around it. This is to confirm that the experiment is working. Interestingly, the test compounds showed no microbial growths on the surface, even though no pronounced inhibition zones were observed around most of the tested membranes samples. What this observation indicates is that the membrane surfaces do, in fact, possess antimicrobial activity. This can, in turn, translate to the decreased susceptibility to membrane surface biofilming and biofouling. The zone of inhibition was measured as shown in Table 2. All the test compounds exhibited activity against *E. coli*. with inhibition zones around 4–7 mm. Interestingly, the 1% HPEI/PES showed quantifiable zone of inhibition against all the five bacterial strains tested. The antibacterial properties of HPEI is very limited in literature, and its mechanism of action is believed to be through the depolarization of the cytoplasmic membrane [23]. Generally, the 2%HPEI/PES membrane samples exhibited the zones of inhibition against the bacterial strains tested. The nAg@HPEI/PES membranes also indicated antibacterial activity against the samples tested. The nAg@1%HPEI/PES membrane samples achieved the highest activity against *E. coli* with an inhibition zone of 7 mm. This occurs when bacteria contacts membrane substrate, and the nAg penetrates the cell membrane, rupturing the negatively charged plasma wall, and this results in cytoxicity. This means that it can kill bacteria and mitigate the formation of biofilms and disrupt existing ones. However, with increasing loadings of HPEI, the zone of inhibition was largely observed to decrease throughout the various bacterial lawns. It is noteworthy that all the nAg@HPEI/PES membrane samples showed better activity against all the five bacterial strains (Figure 8). The membranes were also observed to not discriminate between the gram negative and positive bacteria. This further lends credibility to the antibacterial efficiency against pathogens possessing single and double wall peptidoglycans. This can be attributed to the antibacterial property of nAg in the nanocomposite membrane samples, agreeing with literature [13, 21, 22].

4. Conclusion

New flat sheet membranes possessing both organic antifouling and antibacterial properties were fabricated. The successive modification of PES with HPEI and nAg resulted in enhanced membrane properties in terms of contact angle, pure water fluxes, BSA rejection, and enhanced reversible flux recovery ratio. Additionally, most of the membranes exhibited good antibacterial activities against the bacterial strains tested. Membrane samples with nAg also displayed good antibacterial activities against bacteria E *Coli*. The antibacterial properties indicated by the membranes show great promise in enhancing bacterial resistance, biofilm prevention, and thus antifouling which can lengthen operational lifetime. Worth highlighting, furthermore, is the use of cost friendly HPEI and low levels of modification, and ease of membrane fabrication as reported in this work. The former becomes critical for upscaling to lower production costs. As such, these kinds of membranes could possibly be applied in sustainable wastewater reuse and other water treatment applications.

Declarations

Author contribution statement

Hussein K. Okoro: Author name as it appears on the manuscript: Conceived and designed the experiments; Performed the experiments; Wrote the paper.

Lwazi Ndlwana:Performed the experiments; Analyzed and interpreted the data; Wrote the paper.

Monisola I. Ikhile: Performed the experiments; Analyzed and interpreted the data; Wrote the paper.

Tobias G Barnard: Performed the experiments, analyzed and interpreted the data; Wrote the paper.

J. Catherine Ngila: Contributed reagents, materials, analysis tools or data; Wrote the paper.

Data availability statement

Data will be made available on request.

Declaration of interests statement

The authors declare no conflict of interest.

Additional information

No additional information is available for this paper.

References

[1] H.K. Okoro, J.O. Ige, O.A. Iyiola, J.C. Ngila, Fractionation profile, mobility patterns and correlations of heavy metals in estuary sediments from olonkoro river, in tede catchment of western region, Nigeria, Environ. Nanotechnol. Monit. Manag. 8 (2017) 53–62.

[2] I.E.J. Barnhoorn, J. van Dyk, B. Genthe, W. Harding, G. Wagenaar, M. Bornman, Organochlorine pesticide levels in Clarias gariepinus from polluted freshwater impoundments in South Africa and associated human health risks, Chemosphere 120 (2015) 391–397.

[3] A.a. Burbano, S.S. Adham, W.R. Pearce, The state of full-scale RO/NF desalination—results from a worldwide survey, J. AWWA 99 (2007) 116–127.

[4] A. Prüss-Üstün, World Health Organization, Safer Water, Better Health : Costs, Benefits and Sustainability of Interventions to Protect and Promote Health, Annette Prüss-Üstün ., 2008 [et al], https://apps.who.int/iris/handle/10665/43840.

[5] B.P. Tripathi, N.C. Dubey, S. Choudhury, M. Stamm, Antifouling and tunable amino functionalized porous membranes for filtration applications, J. Mater. Chem. 22 (2012) 19981–19992.

[6] B. Deng, M. Yu, X. Yang, B. Zhang, L. Li, L. Xie, J. Li, X. Lu, Antifouling microfiltration membranes prepared from acrylic acid or methacrylic acid grafted poly(vinylidene fluoride) powder synthesized via pre-irradiation induced graft polymerization, J. Membr. Sci. 350 (2010) 252–258.

[7] G. Mazziotti di Celso, M. Prisciandaro, Wastewater reuse by means of UF membrane process: a comparison with Italian provisions, Desalin. Water Treat. 51 (2013) 1615–1622.

[8] M.G. Mayer, D.N. Wilson, Health and safety—the downward trend in lead levels, J. Power Sources 73 (1998) 17–22.

[9] L. de A. Pereira, I.G. de Amorim, J.B.B. da Silva, Development of methodologies to determine aluminum, cadmium, chromium and lead in drinking water by ET AAS using permanent modifiers, Talanta 64 (2004) 395–400.

[10] Q.W. Yang, W.S. Shu, J.W. Qiu, H.B. Wang, C.Y. Lan, Lead in paddy soils and rice plants and its potential health risk around Lechang Lead/Zinc Mine, Guangdong, China, Environ. Int. 30 (2004) 883–889.

[11] P. Tshindane, P.P. Mamba, L. Moss, U.U. Swana, W. Moyo, M.M. Motsa, N. Chaukura, B.B. Mamba, T.T.I. Nkambule, The occurrence of natural organic matter in South African water treatment plants, J. Water Proc. Engin. 31 (2019) 100809.

[12] M.M. Motsa, B.B. Mamba, A. D'Haese, E.M.V. Hoek, A.R.D. Verliefde, Organic fouling in forward osmosis membranes: the role of feed solution chemistry and membrane structural properties, J. Membr. Sci. 460 (2014) 99–109.

[13] Y. Chen, Y. Zhang, J. Liu, H. Zhang, K. Wang, Preparation and antibacterial property of polyethersulfone ultrafiltration hybrid membrane containing halloysite nanotubes loaded with copper ions, Chem. Eng. J. 210 (2012) 298–308.

[14] A.K. Singh, P. Singh, S. Mishra, V.K. Shahi, Anti-biofouling organic-inorganic hybrid membrane for water treatment, J. Mater. Chem. 22 (2012) 1834–1844.

[15] L. Ndlwana, K. Sikhwivhilu, R.M. Moutloali, J.C. Ngila, Heterogeneous functionalization of polyethersulfone: a new approach for pH-responsive microfiltration membranes with enhanced antifouling properties, J. Memb. Sci. Res. 6 (2020) 178–187.

[16] L. Yan, Y.S. Li, C.B. Xiang, S. Xianda, Effect of nano-sized Al2O3-particle addition on PVDF ultrafiltration membrane performance, J. Membr. Sci. 276 (2006) 162–167.

[17] Y.-F. Yang, H.-Q. Hu, Y. Li, L.-S. Wan, Z.-K. Xu, Membrane surface with antibacterial property by grafting polycation, J. Membr. Sci. 376 (2011) 132–141.

[18] S. Chen, Y. Xie, T. Xiao, W. Zhao, J. Li, C. Zhao, Tannic acid-inspiration and post-crosslinking of zwitterionic polymer as a universal approach towards antifouling surface, Chem. Eng. J. 337 (2018) 122–132.

[19] A. Slistan-Grijalva, R. Herrera-Urbina, J.F. Rivas-Silva, M. Ávalos-Borja, F.F. Castillón-Barraza, A. Posada-Amarillas, Synthesis of silver nanoparticles in a polyvinylpyrrolidone (PVP) paste, and their optical properties in a film and in ethylene glycol, Mater. Res. Bull. 43 (2008) 90–96.

[20] K. Zodrow, L. Brunet, S. Mahendra, D. Li, A. Zhang, Q. Li, P.J.J. Alvarez, Polysulfone ultrafiltration membranes impregnated with silver nanoparticles show improved biofouling resistance and virus removal, Water Res. 43 (2009) 715–723.

[21] H. Basri, A.F. Ismail, M. Aziz, Polyethersulfone (PES)–silver composite UF membrane: effect of silver loading and PVP molecular weight on membrane morphology and antibacterial activity, Desalination 273 (2011) 72–80.

[22] J.A. Prince, S. Bhuvana, V. Anbharasi, N. Ayyanar, K.V.K. Boodhoo, G. Singh, Self-cleaning Metal Organic Framework (MOF) based ultra filtration membranes - a solution to bio-fouling in membrane separation processes, Sci. Rep. 4 (2014).

[23] K.A. Gibney, I. Sovadinova, A.I. Lopez, M. Urban, Z. Ridgway, G.A. Caputo, K. Kuroda, Poly(ethylene imine)s as antimicrobial agents with selective activity, Macromol. Biosci. 12 (2012) 1279–1289.

[24] T. Nada, T. Hodgkiess, NF membranes characterisation: relating performance (flux and rejection) with surface properties (contact angle and surface free energy), Procedia Engineering 44 (2012) 1468–1469.

[25] N.E. Salim, N.A.M. Nor, J. Jaafar, A.F. Ismail, M.R. Qtaishat, T. Matsuura, M.H.D. Othman, M.A. Rahman, F. Aziz, N. Yusof, Effects of hydrophilic surface macromolecule modifier loading on PES/O-g-C3N4 hybrid photocatalytic membrane for phenol removal, Appl. Surf. Sci. 465 (2019) 180–191.

[26] A. Anand, B. Unnikrishnan, J.-Y. Mao, H.-J. Lin, C.-C. Huang, Graphene-based nanofiltration membranes for improving salt rejection, water flux and antifouling–A review, Desalination 429 (2018) 119–133.

[27] P. Kanagaraj, I.M.A. Mohamed, W. Huang, C. Liu, Membrane Fouling Mitigation for Enhanced Water Flux and High Separation of Humic Acid and Copper Ion Using Hydrophilic Polyurethane Modified Cellulose Acetate Ultrafiltration Membranes, Reactive and Functional Polymers, 2020, p. 104538.

[28] L. Ndlwana, K. Sikhwivhilu, R. Moutloali, J.C. Ngila, Microwave-assisted graft synthesis and characterization of poly(methacrylic acid)-grafted polyethersulfone towards dense hydrophilic and low-fouling membranes for water treatment, Phys. Chem. Earth, Parts A/B/C 106 (2018) 107–115.

[29] J.-B. Wu, Y.-F. Lin, J. Wang, P.-J. Chang, C.-P. Tasi, C.-C. Lu, H.-T. Chiu, Y.-W. Yang, Correlation between N 1s XPS binding energy and bond distance in metal amido, imido, and nitrido complexes, Inorg. Chem. 42 (2003) 4516–4518.

[30] H. Wu, Q. Feng, H. Yang, E. Alam, B. Gao, D. Gu, Modified biochar supported Ag/Fe nanoparticles used for removal of cephalexin in solution: characterization, kinetics and mechanisms, Colloid. Surface. Physicochem. Eng. Aspect. 517 (2017) 63–71.

[31] P. Mathumba, A.T. Kuvarega, L.N. Dlamini, S.P. Malinga, Synthesis and characterisation of titanium dioxide nanoparticles prepared within hyperbranched polyethylenimine polymer template using a modified sol–gel method, Mater. Lett. 195 (2017) 172–177.

[32] S.X. Liu, J.-T. Kim, S. Kim, Effect of polymer surface modification on polymer–protein interaction via hydrophilic polymer grafting, J. Food Sci. 73 (2008) E143–E150.

[33] D.E. Vlotman, C.J. Ngila, T. Ndlovu, S.P. Malinga, Hyperbranched polymer integrated membrane for the removal of arsenic(III) in water, J. Membr. Sci. Res. 4 (2018) 53–62.

[34] L.Y. Lafreniere, F.D.F. Talbot, T. Matsuura, S. Sourirajan, Effect of poly(vinylpyrrolidone) additive on the performance of poly(ether sulfone) ultrafiltration membranes, Ind. Eng. Chem. Res. 26 (1987) 2385–2389.

[35] T. Arumugham, R.G. Amimodu, N.J. Kaleekkal, D. Rana, Nano CuO/g-C3N4 sheets-based ultrafiltration membrane with enhanced interfacial affinity, antifouling and protein separation performances for water treatment application, J. Environ. Sci. 82 (2019) 57–69.